

Research and Development of a High Performance Axial Compressor

KATO Dai : Doctor of Engineering, Manager, Advanced Technology Department, Research & Engineering Division, Aero-Engine & Space Operations
PALLOT Guillaume : Advanced Technology Department, Research & Engineering Division, Aero-Engine & Space Operations
SUGIHARA Akio : Manager, Engine Technology Department, Research & Engineering Division, Aero-Engine & Space Operations
AOTSUKA Mizuho : Doctor of Engineering, Manager, Advanced Technology Department, Research & Engineering Division, Aero-Engine & Space Operations

Higher efficiency and higher pressure ratios are required for compressors of aircraft turbo-fan engines in order to achieve a fuel burn reduction. In addition, technical issues related to a smaller core size must be overcome to realize a higher overall pressure ratio and higher bypass ratio of an engine. This paper summarizes the development of axial compressor aerodynamic design technologies that address these subjects, including validation through rig testing. The development of some key structural design technologies to realize the original intent of an aerodynamic design is also described, including higher accuracy variable stator vane actuation, tip clearance reduction, and blade forced response prediction.

1. Introduction

Due to today's more stringent standards on environmental compatibility, such as reduced carbon dioxide emission, and increasing demand from airlines for fuel economy in a time of soaring oil prices, fuel burn reduction is an urgent issue for aircraft turbo-fan engines (shown in Fig. 1). Such engines are one of the main power plants for passenger transportation. In order to reduce fuel burn, improvement in total efficiency or Specific Fuel Consumption (SFC) of the engine must be accomplished along with a reduction in weight. Contributions from aerodynamic design to shorten the axial length of the machine, and application of light-weight materials such as composites are the main means of weight reduction. For improvement of SFC, on the other hand, the Bypass ratio (BPR), Overall Pressure Ratio (OPR), and efficiency of each of the components, including compressors, must be increased. Figure 2 shows the change

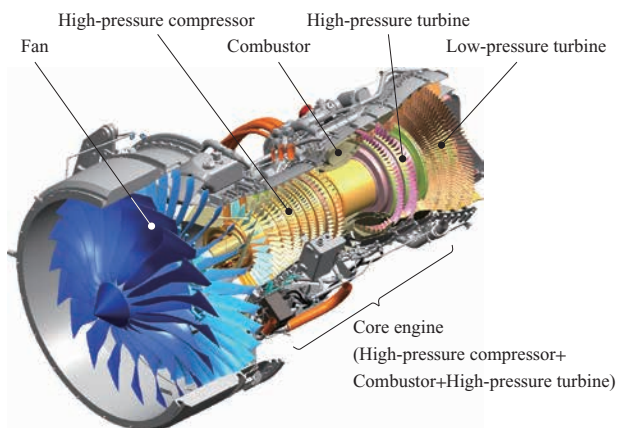


Fig. 1 Turbofan engine (Cutaway model of ECO-engine)

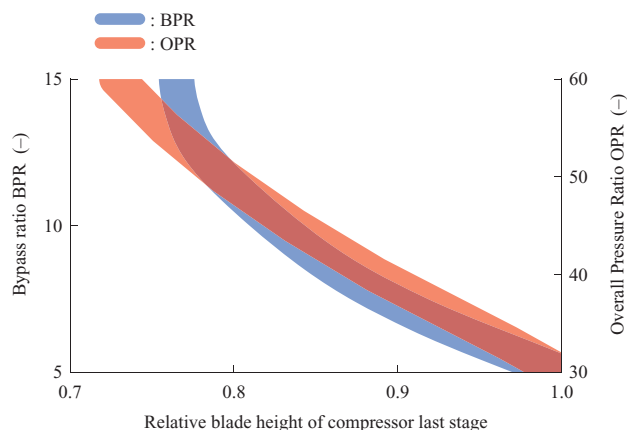


Fig. 2 Compressor blade height variation with BPR and OPR

in the blade height at the last stage of the compressor as BPR and OPR is changed, taking BPR = 5 and OPR = 30 as the baseline. When BPR and OPR are raised to 10 and 50, for example, the last stage blade height shrinks to 64% of the baseline (both factors contributing 80% each). The core size of the engine, which is equivalent to the compressor exit corrected mass flow, becomes smaller accordingly.

In order to address the individual requirements driven by the need for fuel burn reduction of high pressure compressors, namely higher pressure ratio, higher efficiency, and smaller core size, design technologies for high pressure axial compressors have been developed in the Aero-Engine & Space Operations of IHI Corporation. In this article, the developed aerodynamic design technologies are first summarized, including the performance rig test results for a nine-stage compressor. Research and development of the structural design and analysis technologies that support

the realization and improvement of the aerodynamic performance of the machine are then described.

2. Aerodynamic design technology

The aerodynamic design technologies for higher efficiency, higher pressure ratio and an axial compressor with a smaller core size have been addressed in order to realize a higher BPR and OPR. The technology trend of compressor efficiency versus aerodynamic work coefficient is shown in **Fig. 3**.⁽¹⁾ Here, work coefficient is defined as the compressor's total enthalpy rise ($= C_p \times \Delta T$, where C_p is the specific heat at constant pressure and ΔT is the total temperature rise of the compressor) divided by the number of stages Z and the square of the circumferential speed of the rotor at the mean radius, U_m , which is averaged at the compressor inlet and exit. It shows the degree of aerodynamic loading. An increase in load, or a reduction in Z at a constant U_m , reduces the efficiency. Too large of a decrease in load results in an increase in the stage or parts count, which in turn leads to increased acquisition costs, incurring a loss in the competitiveness of the engine. With the emphasis on lower fuel burn, the current trend is for selection of moderate loading. The goal of the present research is to obtain the technologies to design a compressor that is among the most efficient in the world with the moderate load of a 22:1 pressure ratio with nine-stages.

As mentioned before, the blade heights in the rear stages of the compressor decrease as the core size shrinks, resulting in a proportionally larger tip clearance, which is the clearance between the tip of the rotor blades and the inner wall of the casing. In aerodynamics design, a robust technology for minimizing the reduction in performance and operability caused by this clearance enlargement is essential. In the one dimensional design study, work or total enthalpy rise in the rear stage is suppressed for that purpose. Work in the front to mid stages of the machine has to be increased to compensate. The mean radii of these stages are increased to avoid an increase in the work coefficient. These preliminary studies lead to the discovery

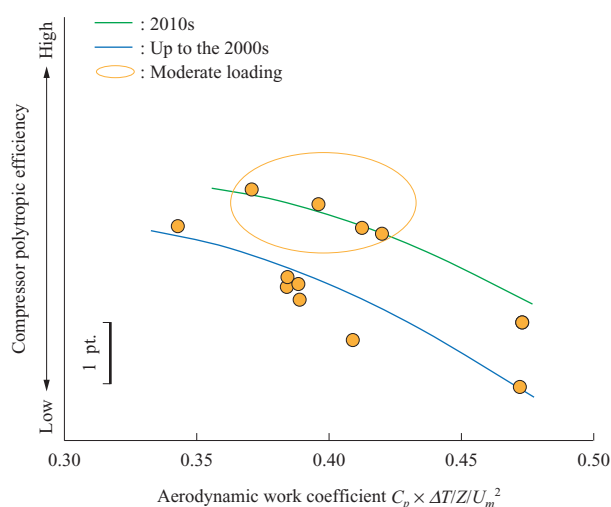


Fig. 3 Compressor efficiency vs. work coefficient

of the flow path and work distribution that fulfill the performance and operability requirements.

The rear stage rotors with a steep pumping characteristic, i.e., a steep increase in pressure ratio with a decrease in the mass flow, are beneficial for the compressor to ensure a stall margin especially at low speeds.⁽²⁾ In the present study, a Diffuser Passage (DP) rotor,^{(2),(3)} which possesses a steeper pumping characteristic and less sensitivity in performance due to tip clearance compared to conventional rotor designs, is employed in the rear two stages of the nine-stage machine. In a conventional rotor, work is accomplished by turning the relative flow through the rotor using an airfoil camber. The tip leakage flow is generated by the local static pressure difference between the suction and pressure sides of the airfoil in accordance with the camber. In the DP rotor, on the other hand, work is done through deceleration of the axial velocity by enlarging the flow path area from the blade's leading edge to the trailing edge, thereby reducing the local camber and the tip leakage flow, see **Fig. 4**.

Three-dimensional designs such as sweep and bow are applied to each of the stages to raise the efficiency.⁽¹⁾ In addition to the effect of the rotor tip clearance, the effect of other real geometries such as the clearance between the casing wall and the Variable Stator Vane (VSV) becomes non-negligible in small compressors. In aerodynamic design, Computational Fluid Dynamic analyses (CFD) are conducted to take these effects into account.⁽²⁾ The main features of the flow path and airfoils are summarized in **Fig. 5**.

In multi-stage compressors, it is important that the operating condition of each stage matches the flow field of the upstream and downstream stages both axially and radially. As shown in **Fig. 6**, an unsteady CFD analysis which simulates the relative motion of the rotor and the stator in the whole nine-stage configuration is conducted in the present study prior to the rig testing to ensure that each of the stages is operating as designed. A modified version of UPACS (Unified Platform for Aerospace Computational Simulation), a compressible Navier-Stokes solver developed by the Japan Aerospace Exploration Agency (JAXA), is employed for this analysis. The modification was made through a collaborative study between JAXA and IHI which enabled UPACS to treat a multi-stage analysis model.

3. Component performance rig test

The entire view of the rotor assembly for the nine-stage compressor is shown in **Fig. 7-(a)**, and a close-up view of the rear stage rotor seen from the compressor exit looking toward the inlet is shown in **Fig. 7-(b)**. As mentioned, swept blade designs are implemented for the front stage rotors, and the low aspect ratio (blade height to blade chord ratio) DP rotor blades are employed in the rear two stages of the assembly. A blisk structure, where the blades and the disk are manufactured as one part, is employed for weight reduction. The external view of the compressor rig installed on the test equipment is shown in **Fig. 8**. Pressure and

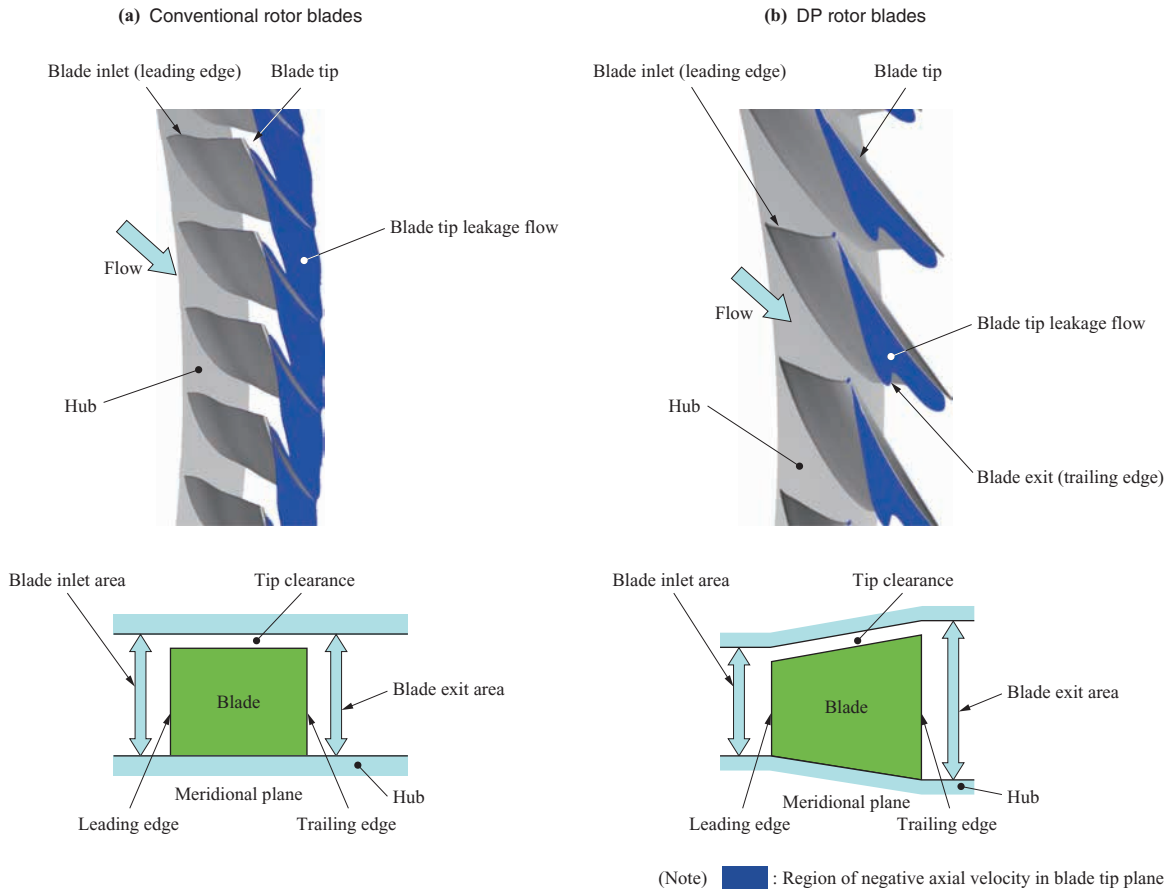


Fig. 4 Suppression of tip leakage flow by DP rotor blades

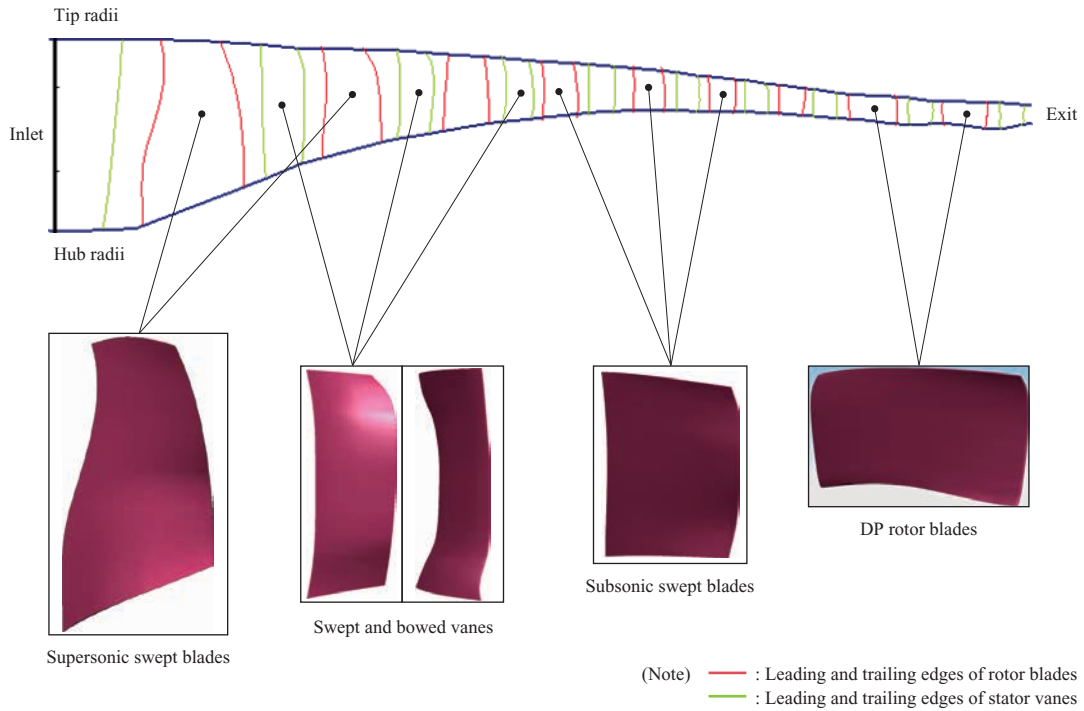
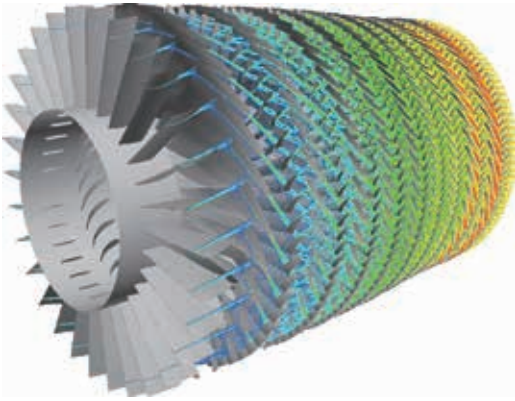


Fig. 5 Aerodynamic flow path and relevant airfoil design features in a nine-stage small core compressor

temperature lines for performance measurement, an actuation device to move VSV's, and bleed pipes for simulating inter-stage bleed in the engine are connected for the component

performance rig test.

The overall test results are shown in Fig. 9. The design mass flow and pressure ratio are obtained at the design



(Note) The entropy at a 90% span is shown as contours.

Fig. 6 All-stage CFD of nine-stage compressor

(a) Whole rotor assembly viewed from upstream



(b) Downstream view of DP rotor blades

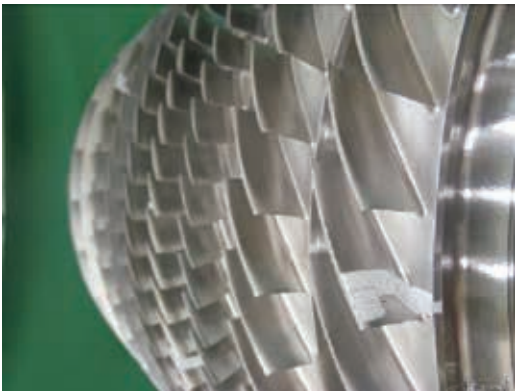


Fig. 7 Rotor assembly of nine-stage compressor

rotor speed. Stage pressure ratios are compared with the design results in Fig. 10. Pressure ratio distribution in the axial direction is fairly close to being as designed, indicating that the operating condition of each stage matches well with the neighboring stages. It should be mentioned that efficiency close to the design goal was also obtained in the rig test.

4. Structural design technology

Research and development for improved VSV angle setting accuracy and reduction in tip clearance will be described

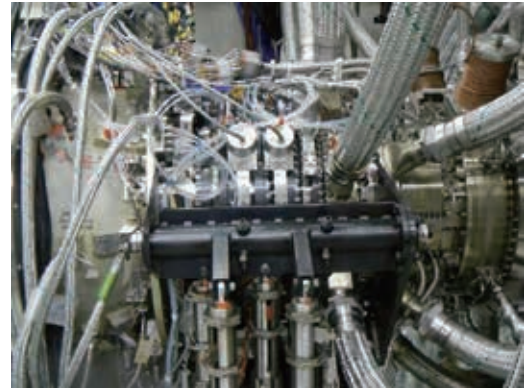


Fig. 8 Compressor rig installed on test facility

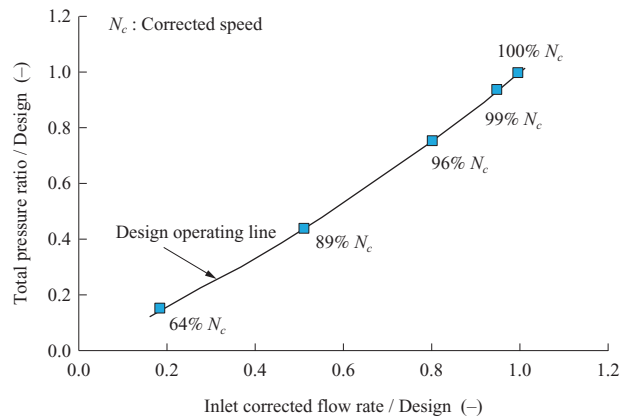
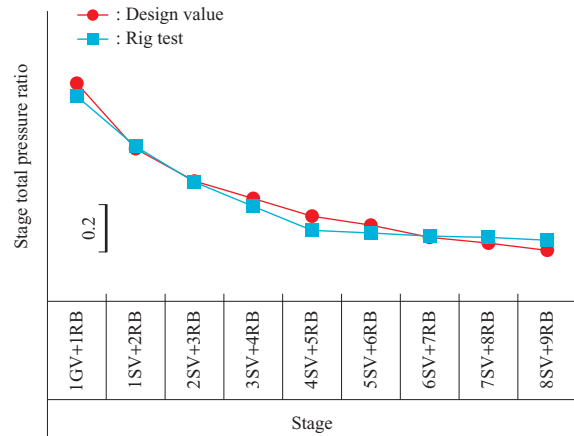


Fig. 9 Overall performance test data of compressor rig



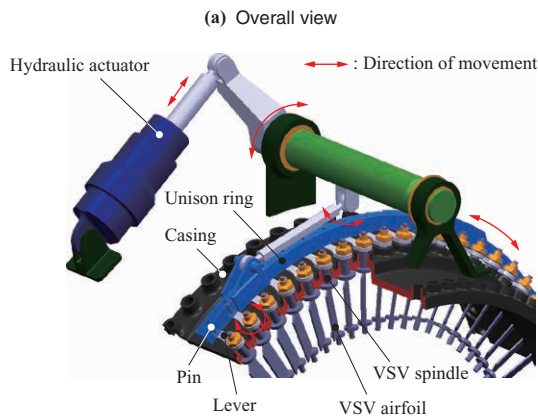
(Note) - 1SV+2RB : Indicates the region between the first stage stator inlet and second stage stator inlet.
 - 1GV+1RB : Indicates the region between the inlet guide vane inlet and first stage stator inlet.

Fig. 10 Measured stage pressure ratio compared to design value

here as examples of structural design technologies that improve compressor performance.

4.1 Improved VSV angle accuracy by optimization of actuation mechanism

A VSV actuation mechanism generally comprises the parts shown in Fig. 11. A rod or a spindle extending radially outward from the VSV airfoil section is inserted through a hole radially bored in the casing. The airfoil section rotates



(b) Casing and Bumpers

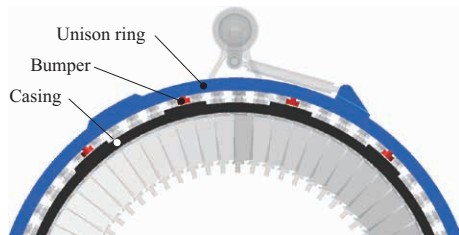


Fig. 11 Example of VSV actuation mechanism

around the spindle and thus the VSV angle setting can be changed. A lever attached to the spindle is pinned to the unison ring. When the ring is rotated around the casing circumferentially, the levers and the VSV airfoils change their orientation in a synchronous manner. The unison ring is connected to the hydraulic actuator, and by controlling the stroke of the actuator, the VSV airfoils can be set to the intended angle.

Also, the unison ring has bumpers with sliding surface materials facing radially inward. The ring can thus rotate concentrically around the casing by sliding on its bumpers over the outer surface of the casing. Maintaining the VSV airfoils uniformly around the circumference at the intended angle will be the main function of this actuation mechanism.

Errors in VSV angle can mainly be reduced by tuning the stiffness of the unison ring, and the number and placement of the bumpers. In order to establish a VSV angle prediction method needed for the tuning, a Multi Body Dynamics (MBD) method was developed. An experimental apparatus like that shown in Fig. 12 was designed and manufactured to validate the MBD method. Elastic deformation of the parts, as well as gaps between the bumpers and the casing are taken into account in this method. The development and validation of the method were jointly conducted with the Research Laboratory of Corporate Research and Development of IHI Corporation.

Taking the stiffness of the ring, the number and the placement of the bumpers as parameters, the error in VSV angle and the load on the actuator were evaluated as outputs. The higher the stiffness of the ring or the higher the number of bumpers, the smaller the error found in VSV angle. At the same time, however, the load and even the instability of

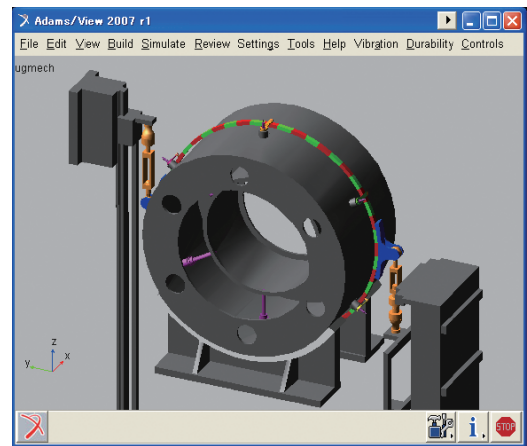


Fig. 12 Analysis model of VSV actuation test stand

the actuator would increase, because the system loses its ability to absorb mechanical unbalance caused by manufacturing tolerances and backlash. It was found that the parameters must be determined in the region where the two factors, the error and the load, satisfy certain design goals. The result of the analysis is shown schematically in Fig. 13.

Recently, it is becoming possible to simultaneously evaluate the structural strength of the actuation system by coupling MBD analysis with the Finite Element Method (FEM) which uses three-dimensional elements. These technologies are being successfully applied to the development of new aircraft engines.

4.2 Tip Clearance reduction by thermal matching

(1) Behavior of the tip clearance during engine operation

As previously mentioned, tip clearance is the small gap between the rotating parts (blades) and the stationary parts (casing), allowing them to move relative to one another as shown in Fig. 14.

From the structural design point of view, it is preferred that tip clearance be as large as possible in order to avoid damage due to rubbing of the rotating parts with the stationary parts. The gap varies during engine operation due to the expansion of the rotating parts by the

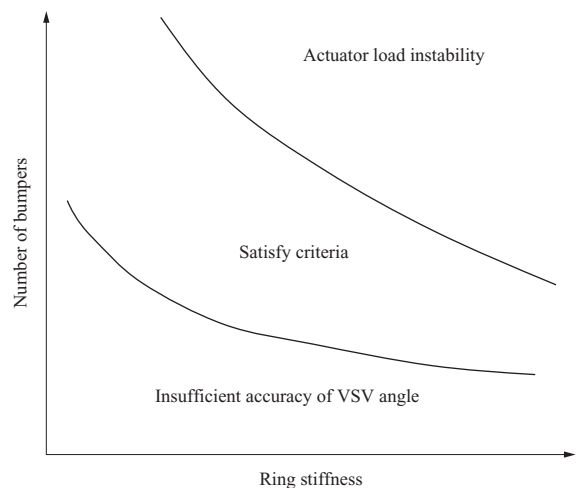


Fig. 13 Relationship between angle accuracy and actuation load

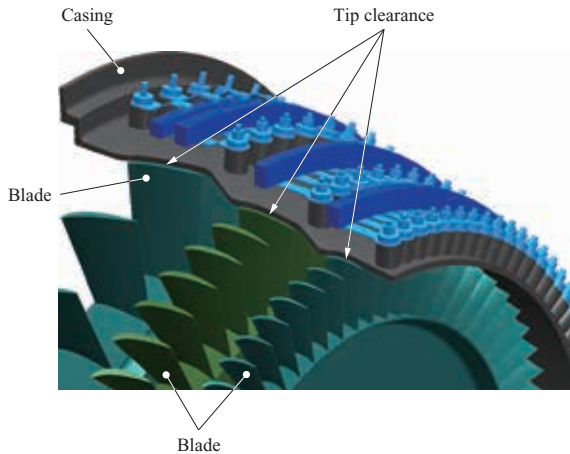


Fig. 14 Tip clearance in axial flow compressor

centrifugal load and due to the thermal expansion of both parts. A small clearance design may result in such contact. On the other hand, from the aerodynamic design point of view, it is preferred that the clearance be as small as possible to minimize blade tip leakage flows, which degrade the performance of the compressor.

To best accommodate both disciplines, it is important to set the tip clearance as small as possible by predicting its behavior accurately and devising structural means to minimize its variance. This prediction becomes highly complicated, since aircraft engines are utilized at various thrust settings from start-up to shut-down, and the environment changes drastically from ground conditions to low temperature, high altitude conditions. For simplicity, a model case is considered here as an example in which the thrust is changed from idle to maximum and back to idle by acceleration and deceleration of the engine. **Figure 15** shows the variation in the amount of expansion of the two parts and the resultant tip clearance. Although there are several factors affecting the amount of expansion, the stationary parts are mostly governed by thermal expansion, the rotating parts by both the centrifugal load and thermal expansion.

The first feature one notices from **Fig. 15** is that the tip clearances tend to enlarge during acceleration. The thermal capacity of the stationary parts or the casing is smaller than the capacity of the rotating parts, i.e. the blades and the disks, and thus the stationary parts respond faster to the temperature change than the

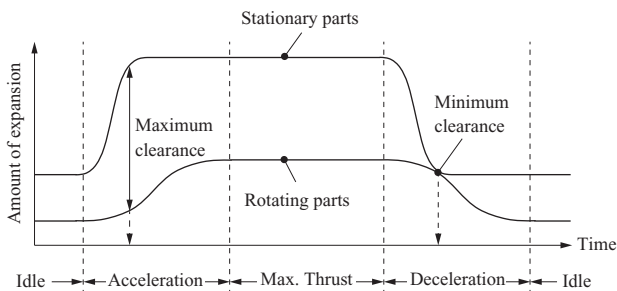


Fig. 15 Tip clearance during basic operation

rotating parts. During deceleration, on the other hand, the clearances tend to narrow rapidly, exposing the parts to a risk of contact failure.

(2) Clearance optimization by thermal matching

Thermal matching is a technique that dampens the increase and decrease of the tip clearance in the transient operation of the engine by adjusting the thermal response of each part. In compressors, this is usually achieved by adding some heat mass to the casing or thickening it to dull its response to temperature changes.

Figure 16 shows an example of thermal matching. By damping the thermal response of the casing, a rapid widening of the clearance is avoided during acceleration, thus improving the performance and stability of the engine. During deceleration, a drastic narrowing of the clearance is also avoided, which is beneficial for the structural reasons described earlier. In the actual design, the tip clearance setting and the amount by which the casing is thickened are determined taking the balance between weight increase and performance improvement into account so that the settings are optimal throughout the engine's mission.

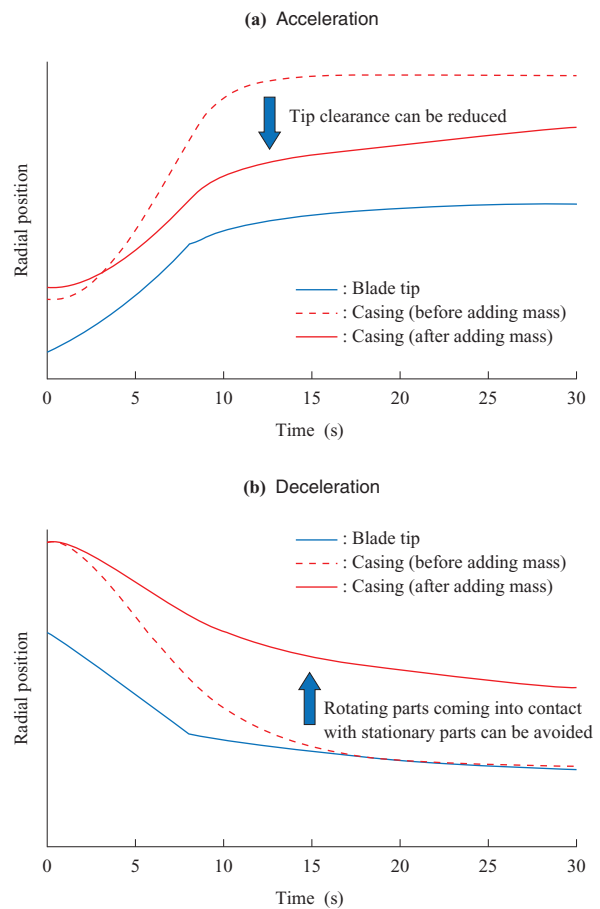


Fig. 16 Effect of heat mass on tip clearance

5. Blade vibratory response prediction technology

It is necessary to detect critical or harmful blade vibrations as early as possible in the development of a compressor, and to take countermeasures to avoid such occurrences. For three-dimensional thin blades in recent engine designs, avoiding the resonances of all of the modes is quite impractical. If the blade vibratory response could be predicted accurately early in the design phase, one would be able to avoid having to redevelop the compressor. In the present study, a blade vibratory response prediction system, often termed a blade forced response prediction system, utilizing three-dimensional unsteady CFD was developed and validated using test data.

The structure of the developed system is shown in **Fig. 17**. Since the aerodynamic excitation force, or the forcing function, is generated by the interaction with the wakes of the upstream vanes or the potential disturbances from either upstream or downstream vanes, an unsteady stage CFD analysis including the blades to be evaluated and the upstream and downstream vanes is conducted. Aerodynamic damping, on the other hand, is generated by the movement of the blades, which are evaluated by themselves. A separate unsteady CFD analysis is performed in which the blades to be evaluated are vibrated with a fixed amplitude in the mode shape of interest. For this purpose, another version of UPACS jointly developed by JAXA and IHI is used in which the blade motion can be simulated. Applying the aerodynamics excitation force and the aerodynamic damping, along with the structural damping from a test database, for example, the magnitude of the blade vibratory response is predicted using the structural response analysis.

The system is validated using vibratory response data of the first stage rotor blade in a six-stage compressor described in Reference (2), in resonance with the IGV wake.⁽⁴⁾ In this compressor, since the first stage rotor is a blisk, the structural damping is considered negligible and is set to zero. A Campbell diagram of this rotor blade is presented in **Fig. 18**. High-order modes called 2-3S, 4F and 5T are excited by the IGV wake at their resonance points. Here,

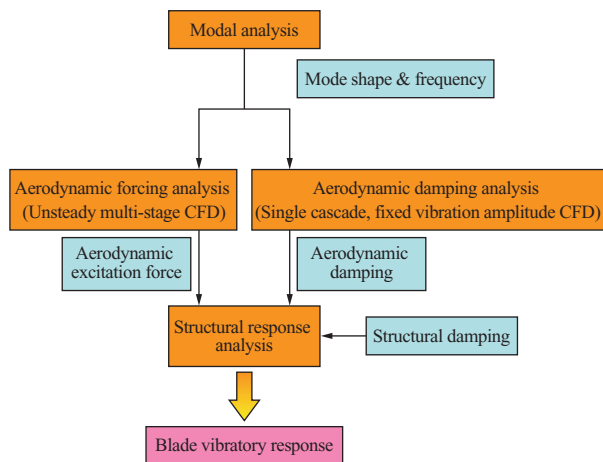


Fig. 17 Forced response prediction system

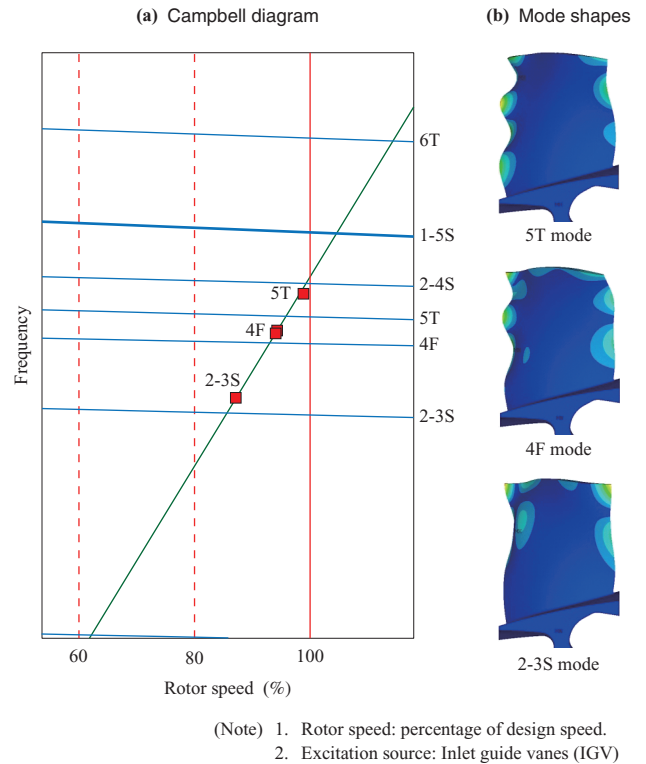


Fig. 18 Campbell diagram and mode shapes

“S” represents chord-wise bending (“S” stands for the Stripe shape of the node of the bending), “F” represents span-wise bending, and “T” represents torsion along the blade stacking axis. And the number in front of these letters shows the order of that vibration type (As also shown by the deformed mode shapes on the right-hand side in **Fig. 18**, “2-3S” means a combination of third order bending in the chord-wise direction and second order bending in the span-wise direction).

Predicted vibratory stresses are compared to the test data in **Fig. 19**. The prediction agrees well with the test data for 2-3S and 5T modes. The discrepancy, on the other hand, is rather large for the 4F mode.

It is demonstrated that the developed prediction system using unsteady CFD has reasonable accuracy for some of

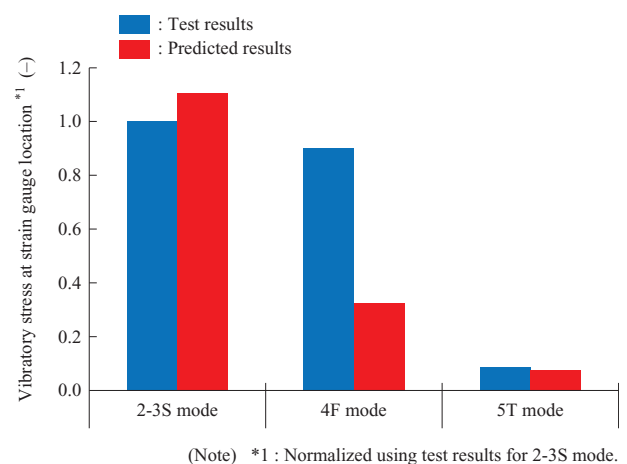


Fig. 19 Predicted vibratory stress compared to test

the vibratory responses. However, it is also shown that for some other cases the prediction error becomes large. In future work, more validations will be conducted to clarify the causes of such discrepancies, and improvements will be made to the system.

6. Conclusion

Research and development activities on high performance compressors of aircraft engines are summarized in this paper. It is stressed that in order to meet the requirements for higher pressure ratios, higher efficiency and smaller core sizes, various advanced aerodynamic design technologies, structural design technologies, and various multi-disciplinary prediction technologies all need enhancement. The competitiveness of IHI's compressor module will be improved steadily by the synergy between such aerodynamic and structural technologies, as well as manufacturing technologies, which are not described in the present paper.

— Acknowledgements —

This study was conducted under contract with the New Energy and Industrial Technology Development Organization (NEDO) as a part of the aircraft and space industry innovation program and the energy innovation program of the Ministry of Economy, Trade and Industry (METI).

The authors would also like to acknowledge the Propulsion Systems Research Group, Institute of Aeronautical Technology of JAXA, for giving us permission to use the versions of UPACS described in this paper.

REFERENCES

- (1) D. Kato : Axial-Flow Compressors for Aircraft Engines Journal of the Gas Turbine Society of Japan Vol. 41 No. 2 (2013. 3) pp. 158-163
- (2) D. Kato, G. Pallot, D. Sato, M. Yamagami and H. Kodama : Development of a Highly Loaded Axial Flow Compressor for Small Core Size Aircraft Engines International Gas Turbine Congress 2011 IGTC2011-0136 (2011. 11) pp. 1-7
- (3) D. Kato, S. Goto, T. Kato, T. Wakabayashi and H. Ochiai : Development of Simple and High-Performance Technology for Compressors IHI Engineering Review Vol. 41 No. 1 (2008. 1) pp. 13-19
- (4) M. Aotsuka, D. Kato and T. Murooka : Numerical Analysis of Forced Response of High Pressure Compressor Cascade The 13th International Symposium on Unsteady Aerodynamics, Aeroacoustics and Aeroelasticity of Turbomachines ISUAAAT13-S2-3 (2012. 9) pp. 1-5